

This is the accepted manuscript made available via CHORUS. The article has been published as:

Steady-state superconductivity in electronic materials with repulsive interactions

O. Hart, G. Goldstein, C. Chamon, and C. Castelnovo

Phys. Rev. B **100**, 060508 — Published 30 August 2019

DOI: [10.1103/PhysRevB.100.060508](https://doi.org/10.1103/PhysRevB.100.060508)

Steady-state superconductivity in electronic materials with repulsive interactions

O. Hart,¹ G. Goldstein,^{1,2} C. Chamon,³ and C. Castelnovo¹

¹*T.C.M. Group, Cavendish Laboratory, J.J. Thomson Avenue, Cambridge CB3 0HE, United Kingdom*

²*Physics and Astronomy Department, Rutgers University, Piscataway, NJ 08854, USA*

³*Physics Department, Boston University, Boston, Massachusetts 02215, USA*

(Dated: October 2018)

We study the effect of laser driving on a minimal model for a hexagonal two-dimensional material with broken inversion symmetry. Through the application of circularly polarised light and coupling to a thermal free electron bath, the system is driven into a nonequilibrium steady state with asymmetric, nonthermal carrier populations in the two valleys. We show that, in this steady state, interband superconducting correlations between electrons can develop independent of the sign of the electronic interactions. We discuss how our results apply, for example, to transition metal dichalcogenides. This work opens the door to technological applications of superconductivity in a range of materials that were hitherto precluded from it.

The use of light to manipulate quantum matter, or even induce phases not present in a given system in equilibrium, is a long-standing area of research that has received renewed attention due to recent theoretical and experimental advances. Notable examples include ultrafast pump-probe spectroscopy [1] and periodic Floquet driving [2–4]. The investigation of superconductivity in particular has often been at the forefront of these efforts [5], beginning in the 1960s with the Wyatt–Dayem effect: experiments on thin metallic films showed that irradiation with sub-gap microwaves gives rise to an increase in the superconducting gap, the critical current, and the critical temperature [6, 7]. Eliashberg [8] showed that these effects could be attributed to a redistribution of quasiparticles in response to the driving. Subsequent experiments showed that this mechanism could in fact lead to superconducting gaps considerably in excess of their equilibrium values [9–12]. In recent years, superconducting order has been shown to develop following femtosecond laser pulses in the cuprates [13–16] and in K_3C_{60} [17] (for an overview, see Ref. [18]).

Photoinduced superconductivity in undoped semiconductors, in which the phenomenon is absent in equilibrium, has been proposed for intraband [20–24] and interband [25] pairing; in the former the superconducting pairing is unstable, and in the latter a delicate fine tuning and assumptions about the electronic dispersion are needed. In this letter we propose a robust mechanism for interband superconductivity which leads to nonzero superconducting correlations without such restrictive requirements, and irrespective of the sign of the interactions between the constituent particles. The mechanism relies only on a few simple ingredients: (i) a bandstructure with two valleys that may be driven independently; (ii) an interband pairing interaction; and (iii) some form of dissipation to reach a nonequilibrium steady state.

These ingredients are naturally realised, for example, in systems with a gapped graphene-like dispersion [26], such as monolayer group-VI transition metal dichalcogenides (TMDs) in the 2H phase. These materials host

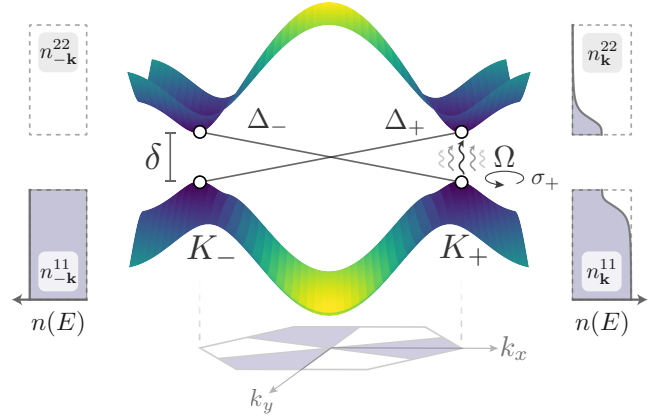


FIG. 1. Schematic illustration of the pairing mechanism. The valley K_+ is driven with σ_+ polarised light of frequency $\omega_0 \simeq \delta$, the bandgap, leading to a nonthermal population of the single-particle states near the centre of the valley. By virtue of broken inversion symmetry, valley K_- is left unaffected by the laser. This induces a nontrivial population difference between the upper and lower bands at $\pm \mathbf{k}$. The corresponding occupations of the two valleys, $n(E)$, are illustrated qualitatively on their respective sides of the figure [19]. Our results show that one of the two pairing channels, Δ_+ or Δ_- , represented symbolically by the solid lines connecting the open circles, is always nonvanishing for sufficiently large Ω .

two inequivalent but degenerate (due to time reversal symmetry) valleys at opposite edges of their hexagonal Brillouin zone (BZ) [27]. It was shown experimentally that the carrier populations in the two valleys can be tuned individually using circularly polarised light [28–30], an effect known as circular dichroism. We argue that photoinduced superconductivity is within reach of state of the art experiments on TMDs and related materials, providing the enticing opportunity to realise it in an altogether new setting where it is not present in equilibrium.

Model.—We focus on the relevant nearest-neighbour tight-binding model on a hexagonal lattice with Hamilto-

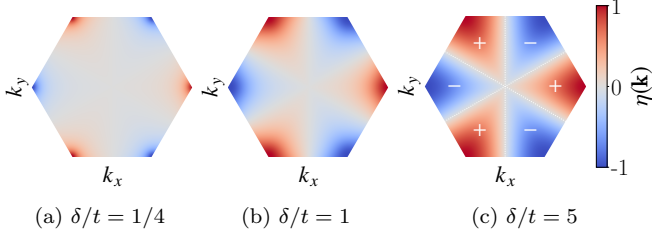


FIG. 2. The asymmetry, quantified by $\eta(\mathbf{k})$, between absorption of light with circular polarisation σ_+ ($\eta = 1$) and σ_- ($\eta = -1$). The valleys K_{\pm} , centered on $\mathbf{K}_{\pm} = \pm \frac{4\pi}{3\sqrt{3}}\mathbf{x}$, couple only to σ_{\pm} polarisations, respectively. The plot is calculated for hexagonal materials described by the Hamiltonian (1) (see Supplemental Material).

nian

$$H(\mathbf{k}) = \begin{pmatrix} \delta/2 & h(\mathbf{k}) \\ h^*(\mathbf{k}) & -\delta/2 \end{pmatrix}, \quad (1)$$

where $h(\mathbf{k}) = -t \sum_i e^{i\mathbf{k} \cdot \mathbf{d}_i}$, the vectors $\mathbf{d}_{1,2} = \frac{a}{2}\mathbf{y} \pm \frac{\sqrt{3}a}{2}\mathbf{x}$, $\mathbf{d}_3 = -a\mathbf{y}$ connect nearest neighbours [26], and $\delta > 0$ represents a staggered chemical potential. We henceforth set the distance between neighbouring atoms $a = 1$. The band structure $E_{\mathbf{k}\alpha}$ corresponding to (1) has two bands ($\alpha = 1, 2$, valence and conduction) separated by a gap δ . The familiar Dirac cones of graphene, centred at $\mathbf{K}_{\pm} = \pm \frac{4\pi}{3\sqrt{3}}\mathbf{x}$, become gapped valleys in the presence of the staggered chemical potential. At the Dirac points K_{\pm} , there is an exact selection rule for optical band-edge transitions: circularly polarised light with polarisation σ_{\pm} couples only to transitions within the K_{\pm} valley [31]. Hence, each valley can be driven independently.

This asymmetry between absorption of σ_{\pm} polarisations is quantified by the degree of circular polarisation [30, 31],

$$\eta(\mathbf{k}) = \frac{|\mathcal{P}_+^{21}(\mathbf{k})|^2 - |\mathcal{P}_-^{21}(\mathbf{k})|^2}{|\mathcal{P}_+^{21}(\mathbf{k})|^2 + |\mathcal{P}_-^{21}(\mathbf{k})|^2}, \quad (2)$$

where $\mathcal{P}_{\pm}^{21}(\mathbf{k}) = \langle \psi_{2\mathbf{k}} | p_{\pm} | \psi_{1\mathbf{k}} \rangle$ and $p_{\pm} = p_x \pm ip_y$ describe optical transitions between the two bands. The asymmetry, calculated using (1), is plotted for various staggered chemical potentials over the first BZ in Fig. 2. It is exact ($\eta = \pm 1$) at \mathbf{K}_{\pm} [31], and spreads towards the centre of the BZ for $\delta \gtrsim t$. The driving strength is parameterised in terms of the Rabi frequency $\Omega_{\mathbf{k}} = (eE_0/2m\omega_0)\mathcal{P}_{\pm}^{21}(\mathbf{k})$, which we take to be real. E_0 , e and m describe the strength of the electric field and the electronic charge and mass, respectively.

We study two limiting cases: (i) when relaxation occurs exclusively through tunnel coupling to a three-dimensional substrate, and (ii) when fast intraband relaxation establishes a local equilibrium in the upper and lower bands separately. The latter case is important for its closer connection to experiment, but the derivation of the results

uses a more phenomenological approach that is easier to follow after exposure to the results of the former. Hence, we focus first on case (i) where we are able to confirm our results using two separate methods. The details of case (ii) are presented in the Supplemental Material.

We assume a simplified driving pattern as a minimal model of σ_+ polarised driving in which $\Omega_{\mathbf{k}} = \Omega$ in the regions of the first BZ where $\eta(\mathbf{k}) > 0$ in Fig. 2c, and $\Omega_{\mathbf{k}} = 0$ where $\eta(\mathbf{k}) < 0$. These two regions will be referred to as $\mathbf{k} \in K_{\pm}$, respectively. Although the Rabi frequency in any real material depends continuously on momentum, in practice this dependence may be neglected since the dominant contribution to the superconducting gap equation comes from the vicinity of the surface $S_{\omega_0} = \{\mathbf{k} : E_{\mathbf{k}2} - E_{\mathbf{k}1} = \omega_0\}$ where the laser is resonant.

Our complete model Hamiltonian is composed of an interacting system (S), a bath (B), and a system–bath (S–B) interaction $H = H_S + H_{\text{int}} + H_{S-B} + H_B$, where

$$H_S = \sum_{\lambda} E_{\lambda} c_{\lambda}^{\dagger} c_{\lambda} + \sum_{\mathbf{k}} \Omega_{\mathbf{k}} (e^{i\omega_0 t} c_{\mathbf{k}2}^{\dagger} c_{\mathbf{k}1} + e^{-i\omega_0 t} c_{\mathbf{k}1}^{\dagger} c_{\mathbf{k}2}), \quad (3)$$

$$H_{\text{int}} = \frac{1}{N} \sum_{\mathbf{k}, \mathbf{k}'} V_{\mathbf{k}\mathbf{k}'} c_{\mathbf{k}2}^{\dagger} c_{-\mathbf{k}1}^{\dagger} c_{-\mathbf{k}'1} c_{\mathbf{k}'2}, \quad (4)$$

$$H_{S-B} = \sum_{\lambda, n} t_{\lambda} (c_{\lambda}^{\dagger} a_{\lambda n} + a_{\lambda n}^{\dagger} c_{\lambda}), \quad (5)$$

$$H_B = \sum_{\lambda, n} \omega_{\lambda n} a_{\lambda n}^{\dagger} a_{\lambda n}. \quad (6)$$

The index $\lambda = (\mathbf{k}, \alpha)$ labels the noninteracting system modes, and N is the number of unit cells. Both the system and the bath are composed of spinless fermions: $\{c_{\lambda}, c_{\lambda'}^{\dagger}\} = \delta_{\lambda\lambda'}$, and $\{a_{\lambda n}, a_{\lambda' m}^{\dagger}\} = \delta_{\lambda\lambda'} \delta_{nm}$ [32]. The system is driven by a laser of frequency ω_0 , and interacts via the scattering of interband pairs [33]. Coupling the system to a bath with which it can exchange both energy and particles brings our system towards a unique nonequilibrium steady state [34].

Born–Markov approximation.—The simplest possible analysis of our time-dependent Hamiltonian can be performed by moving into the frame rotating at ω_0 and applying the Born–Markov approximation. In this approach, we assume that the baths have a continuous density of states $\nu_{\lambda}(\epsilon)$, and that they interact weakly with the system: $|t_{\lambda}|^2 \nu_{\lambda} \ll \delta$. The dynamics of the system S, described by its reduced density matrix $\rho_S = \text{Tr}_B \rho$, is then determined approximately [35] by the Master equation [36]

$$\begin{aligned} \frac{d\rho_S}{dt} = & -i[H_S, \rho_S] + \sum_{\lambda} \Gamma_{\lambda} \{n_F(\xi_{\lambda}) \mathcal{D}[c_{\lambda}^{\dagger}] \rho_S \\ & + [1 - n_F(\xi_{\lambda})] \mathcal{D}[c_{\lambda}] \rho_S\}, \end{aligned} \quad (7)$$

where $n_F(\xi) = (1 + e^{\beta\xi})^{-1}$ is the Fermi–Dirac distribution, $\xi_{\lambda} = E_{\lambda} - \mu$, and the rates $\Gamma_{\lambda} = 2\pi |t_{\lambda}|^2 \nu_{\lambda}(\xi_{\lambda})$ are given

by Fermi's golden rule. The Lindbladian dissipators \mathcal{D} are defined as $\mathcal{D}[X]\rho = (2X\rho X^\dagger - X^\dagger X\rho - \rho X^\dagger X)/2$. We have neglected any Lamb shift corrections to (7) which renormalise the bandstructure E_λ [37]. We will henceforth assume that both bands are characterised by momentum-independent rates $\Gamma_\lambda \rightarrow \Gamma_\alpha$, $\alpha = 1, 2$.

After making a mean field approximation for the superconducting order parameter in (4), we can write down the equations of motion for the populations and correlators, $n_{\mathbf{k}}^{\alpha\beta}(t) = \langle c_{\mathbf{k}\alpha}^\dagger c_{\mathbf{k}\beta} \rangle$ and $s_{\mathbf{k}}^{\alpha\beta}(t) = \langle c_{\mathbf{k}\alpha}^\dagger c_{-\mathbf{k}\beta}^\dagger \rangle$, and solve for the steady state in the long-time limit (typically, $t \gg \Gamma_1^{-1}, \Gamma_2^{-1}$). One may then substitute the steady-state value for the anomalous correlator $s_{\mathbf{k}}^{21}$ into the self-consistency condition

$$\Delta_{\mathbf{k}} = \frac{1}{N} \sum_{\mathbf{k}'} V_{\mathbf{k}\mathbf{k}'} \langle c_{-\mathbf{k}'1} c_{\mathbf{k}'2} \rangle. \quad (8)$$

We make the following simplifying assumption about the scattering amplitudes $V_{\mathbf{k}\mathbf{k}'}$: there exist only two relevant average scattering amplitudes V and $V' = ve^{i\phi}$ which, respectively, correspond to intra- ($K_\pm \rightarrow K_\pm$) and intervalley ($K_\mp \rightarrow K_\pm$) scattering events. This in turn implies that there are only two momentum components of the gap, Δ_\pm , corresponding to momenta in the vicinity of valley K_\pm . These two amplitudes will satisfy $|V| \gg |V'|$; since the two valleys are separated by a large momentum transfer, intervalley scattering events are strongly suppressed with respect to intravalley events [indeed, one may show that $V' = V \sum_{\mathbf{d}} e^{2i\mathbf{K} \cdot \mathbf{d}}/3 = 0$ identically using the eigenstates of $H(\mathbf{k})$ in (1) for scattering between the valley centres]. Using the Born-Markov equations of motion derived from (7), we obtain that

$$\begin{aligned} \bar{\Delta}_\pm &= -\bar{\Delta}_\pm \frac{V}{N} \sum_{\mathbf{k} \in K_\pm} \frac{E_{\mathbf{k}}}{E_{\mathbf{k}}^2 + \Gamma^2} (1 - n_{\mathbf{k}}^{22} - n_{-\mathbf{k}}^{11}) \\ &\quad - \bar{\Delta}_\mp \frac{ve^{\pm i\phi}}{N} \sum_{\mathbf{k} \in K_\mp} \frac{E_{\mathbf{k}}}{E_{\mathbf{k}}^2 + \Gamma^2} (1 - n_{\mathbf{k}}^{22} - n_{-\mathbf{k}}^{11}), \end{aligned} \quad (9)$$

which is to be contrasted with the standard BCS self-consistency condition [38]; the equilibrium populations have been replaced by their nonequilibrium counterparts. We have defined $E_{\mathbf{k}} = \xi_{\mathbf{k}1} + \xi_{\mathbf{k}2}$, $\epsilon_{\mathbf{k}} = \xi_{\mathbf{k}2} - \xi_{\mathbf{k}1} - \omega_0$ and $\Gamma = \Gamma_1 + \Gamma_2$. Note that (9) reduces to the standard self-consistency condition when $\Gamma \rightarrow 0^+$, as it must.

In writing down (9), we have made the assumption that the damping Γ is small. If Γ is increased in magnitude, the gap parameters acquire an oscillatory time dependence, i.e., a modification of the effective system chemical potential [39, 40]. If Γ is made sufficiently large, superconducting order is eventually destroyed [41]. Driving the valley K_+ with circularly polarised light σ_+ , we find the following steady-state populations for momenta $\mathbf{k} \in K_+$

and $\Delta_\pm = 0$

$$n_{-\mathbf{k}}^{22} = n_{\mathbf{k}}^2, \quad n_{\mathbf{k}}^{22} = \frac{n_{\mathbf{F}}^2 + \tilde{\Omega}_{\mathbf{k}}^2(n_{\mathbf{F}}^1/\gamma_2 + n_{\mathbf{F}}^2/\gamma_1)}{1 + \tilde{\Omega}_{\mathbf{k}}^2(1/\gamma_2 + 1/\gamma_1)}, \quad (10)$$

$$n_{-\mathbf{k}}^{11} = n_{\mathbf{F}}^1, \quad n_{\mathbf{k}}^{11} = \frac{n_{\mathbf{F}}^1 + \tilde{\Omega}_{\mathbf{k}}^2(n_{\mathbf{F}}^1/\gamma_2 + n_{\mathbf{F}}^2/\gamma_1)}{1 + \tilde{\Omega}_{\mathbf{k}}^2(1/\gamma_2 + 1/\gamma_1)}, \quad (11)$$

where $n_{\mathbf{F}}^\alpha \equiv n_{\mathbf{F}}(\xi_{\mathbf{k}\alpha})$, $\tilde{\Omega}_{\mathbf{k}}^2 \equiv \Omega^2/(\epsilon_{\mathbf{k}}^2 + \Gamma^2)$, and $\gamma_\alpha = \Gamma_\alpha/\Gamma$. That is, the valley K_- is unaffected by the laser drive, while the populations in the valley K_+ are nonthermal. We note that adding an intervalley scattering term to the equations of motion (7), in which intervalley scattering events occur with rate Γ_s , does not significantly alter the nonequilibrium populations as long as $\Gamma_s \ll \Gamma$, as shown in the Supplemental Material.

The nonequilibrium gap equation (9) may be written in matrix form as

$$\begin{pmatrix} \Delta_+ \\ \Delta_- \end{pmatrix} = \begin{pmatrix} VF_+ & ve^{i\phi}F_- \\ ve^{-i\phi}F_+ & VF_- \end{pmatrix} \begin{pmatrix} \Delta_+ \\ \Delta_- \end{pmatrix}. \quad (12)$$

Including further scattering amplitudes simply increases the dimensionality of this matrix. To zeroth order in $|V'|/|V|$, the onset of superconductivity is determined solely by the behaviour of the two functions F_\pm with increasing driving strength

$$F_\pm \equiv -\frac{1}{N} \sum_{\mathbf{k} \in K_\pm} \frac{E_{\mathbf{k}}}{E_{\mathbf{k}}^2 + \Gamma^2} (1 - n_{\mathbf{k}}^{22} - n_{-\mathbf{k}}^{11}). \quad (13)$$

The induced population differences $1 - n_{\mathbf{k}}^{22} - n_{-\mathbf{k}}^{11}$ for $\mathbf{k} \in K_+$ and $\mathbf{k} \in K_-$ have *opposite* sign, which is inherited by the functions F_+ and F_- . Equation (13) justifies our focus on interband pairing. In equilibrium, at temperatures $T \ll \delta$, the population difference $1 - n_{\mathbf{k}}^{22} - n_{-\mathbf{k}}^{11}$ approximately vanishes. Therefore the occupations, $n_{\mathbf{k}}^{\alpha\alpha}$, need only be modified slightly by driving in order to change the sign of the nonequilibrium population difference, allowing for the possibility of superconductivity in the presence of repulsive interactions [42]. Further, the electronic bands satisfy the resonance condition $E_{\mathbf{k}} \simeq 0$. Substituting in the steady-state values of the populations and defining $\bar{\gamma}^{-1} = \gamma_1^{-1} + \gamma_2^{-1}$, we arrive at

$$F_+ = \frac{1}{2\gamma_2} \frac{-\mu}{\mu^2 + (\Gamma/2)^2} \int dE \rho(E) \frac{\Omega^2}{\epsilon(E)^2 + \Omega^2/\bar{\gamma} + \Gamma^2}, \quad (14)$$

$$F_- = -\frac{\gamma_2}{\gamma_1} F_+, \quad (15)$$

for temperatures $T \ll \delta$. The domain of integration extends over positive energies only. The density of states per unit cell $\rho(E)$ for hexagonal materials described by Eq. (1) can be evaluated exactly in terms of the corresponding gapless density of states ρ_0 : $\rho(E) = (E/\tilde{E})\rho_0(\tilde{E})/4$, where $\tilde{E} = \sqrt{E^2 - (\delta/2)^2}$ [43] (the factor of 4 removes spin and valley degeneracy). Hereafter we will simplify

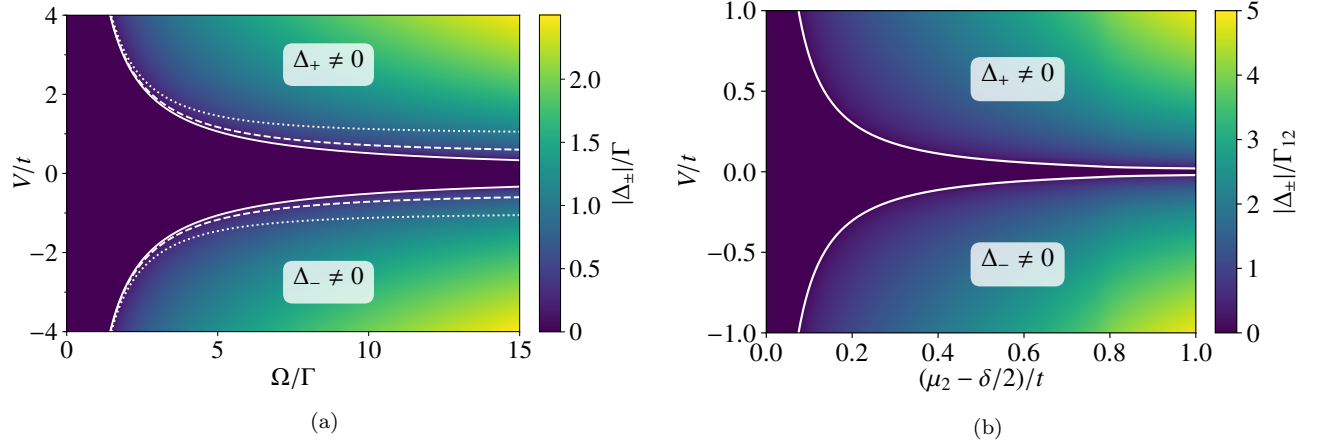


FIG. 3. (a) Critical coupling V_c , in units of the hopping integral t , as a function of driving strength, parameterised by the Rabi frequency Ω . There are two branches; one positive and one negative, which means that superconductivity may develop irrespective of the sign of interactions V . For sufficiently large driving (with respect to the damping Γ), the critical coupling saturates to $|V'|$, the intervalley scattering matrix element. $V'/t = 0, 1/2, 1$ correspond to the solid, dashed and dotted lines, respectively. If $V' = 0$ (the value used for the colourmap) then only one of Δ_+ or Δ_- is nonzero. A bandgap of $\delta/t = 5$, damping rates $\Gamma_1 = \Gamma_2 = 10^{-3}t$ and chemical potential $\mu = -\Gamma/2$ were used for the plot. (b) The equivalent plot for the case of fast intraband relaxation with rate Γ_{12} . The population difference $1 - n_{\mathbf{k}}^{22} - n_{\mathbf{k}}^{11}$ is now controlled by μ_2 , an effective chemical potential which determines the nonequilibrium populations of the K_+ valley. The parameters used for the plot are $\delta/t = 1/4$, $\Gamma_{12} = 10^{-3}t$ and $\mu = -\Gamma_{12}/2$, implying that $\mu_2/t \simeq 0.2$ corresponds to 2.6% polarisation of the K_+ valley.

to the symmetric choice $\gamma_1 = \gamma_2$, in which case we find that $F_- = -F_+$. In the presence of a finite intervalley coupling $v = |V'|$, the equation determining the onset of superconductivity reads

$$1 = (V^2 - v^2)F_+^2. \quad (16)$$

This expression represents our central result: (16) is *insensitive to the sign* of V , and therefore always has a solution as long as the driving is sufficiently strong. This result is illustrated by the phase diagram in Fig. 3a. The two branches with opposite signs indicate that a solution is possible for both attractive and repulsive V [44]. For nonzero V' , the critical $|V|$ does not tend to zero in the limit of large driving strengths, but instead saturates at a value $V_c = \pm|V'|$. Evidently, then, it is desirable to have $|V'|$ be as small as possible, which, as we have discussed, is automatically the case in real materials.

Ideal parameters.—The benefit of the simplified Born–Markov approach is that we are able to evaluate expressions explicitly, which allows us to make concrete statements about optimising the system parameters in order to minimise V_c . It is evident from (14) that the chemical potential should be chosen to be as close to $\pm\Gamma/2$ as possible. Assuming this optimal setup $\mu = -\Gamma/2$, F_{\pm} in (14) evaluates approximately to

$$F_{\pm} \simeq \pm \frac{A_c}{36t} \frac{\delta}{t} \frac{(\Omega/\Gamma)^2}{\sqrt{1 + 4(\Omega/\Gamma)^2}}, \quad (17)$$

for $t \gtrsim \delta \gg \Omega, \Gamma$, neglecting subleading corrections. $A_c = 3\sqrt{3}/2$ is the area of one unit cell. This expression

suggests that one should (i) maximise the ratio δ/t , which has the additional benefit of increasing the validity of our assumption about the driving pattern (see Fig. 2); and (ii) minimise Γ so that the physics of interest occurs at a lower laser power. It should be noted however that the magnitude of the gap also depends on Γ (through $\Delta/\Gamma \sim \sqrt{\Omega/\Gamma}$ for $\Omega \gg \Gamma$) so a smaller damping rate also corresponds to a smaller superconducting gap.

Fast intraband relaxation.—When the interband relaxation rate is slow with respect to the intraband rate Γ_{12} , the upper and lower bands (in the valley K_+) will separately equilibrate to quasithermal distributions with effective chemical potentials μ_2 and μ_1 , respectively. These are determined by the driving strength in addition to the intraband relaxation rate and particle number conservation. (The gap equations for this regime are presented in the Supplemental Material.) The phase diagram for this limiting case is shown in Fig. 3b, and is to be contrasted with its counterpart, Fig. 3a. Importantly, the two branches for V_c with opposite sign persist in this limit. Quantitatively, however, the critical coupling strengths are significantly smaller by virtue of a larger induced population difference. Therefore, this regime where interband relaxation is slower than intraband relaxation, which is closer to the situation in real experiments, coincides with the case where superconductivity with repulsive interactions is most favorable.

Outlook.—We have shown that two-dimensional materials exhibiting circular dichroism can be driven to a superconducting instability due to interband pairing, re-

ardless of the sign of electronic interactions. We demonstrated this mechanism for two limiting cases of dissipation. We also showed in the Supplemental Material that qualitatively similar results are obtained using a more complete Keldysh description of the problem. Our results are of direct relevance to the monolayer transition metal dichalcogenides, which satisfy the criteria outlined in this letter.

This opens the possibility of turning a range of insulating materials into superconductors at the flip of a switch.

Acknowledgements.—The authors would like to thank Camille Aron for useful discussions. This work was supported in part by Engineering and Physical Sciences Research Council (EPSRC) Grants No. EP/P034616/1 and No. EP/M007065/1 (C.Ca. and O.H.), by NSF grant No. DMR-1733071 (G.G.), and by DOE Grant No. DE-FG02-06ER46316 (C.Ch.). C.Ch. acknowledges the kind hospitality of Trinity College, where this work started while visiting as a Fellow Commoner (of no common rate).

-
- [1] R. Mankowsky, M. Först, and A. Cavalleri, *Reports on Progress in Physics* **79**, 064503 (2016).
 - [2] T. Oka and S. Kitamura, *Annual Review of Condensed Matter Physics* **10**, 387 (2019).
 - [3] A. Eckardt, *Rev. Mod. Phys.* **89**, 011004 (2017).
 - [4] N. Goldman and J. Dalibard, *Phys. Rev. X* **4**, 031027 (2014).
 - [5] D. Langenberg and A. Larkin, *Nonequilibrium superconductivity*, Modern problems in condensed matter sciences (North-Holland, 1986).
 - [6] A. F. G. Wyatt, V. M. Dmitriev, W. S. Moore, and F. W. Sheard, *Phys. Rev. Lett.* **16**, 1166 (1966).
 - [7] A. H. Dayem and J. J. Wiegand, *Phys. Rev.* **155**, 419 (1967).
 - [8] G. Eliashberg, *JETP Lett.* **11**, 114 (1970).
 - [9] J. A. Pals and J. Dobben, *Phys. Rev. B* **20**, 935 (1979).
 - [10] M. G. Blamire, E. C. G. Kirk, J. E. Evetts, and T. M. Klapwijk, *Phys. Rev. Lett.* **66**, 220 (1991).
 - [11] D. R. Heslinga and T. M. Klapwijk, *Phys. Rev. B* **47**, 5157 (1993).
 - [12] P. V. Komissinski and G. A. Ovsyannikov, *Phys. Rev. B* **54**, 13184 (1996).
 - [13] D. Fausti, R. I. Tobey, N. Dean, S. Kaiser, A. Dienst, M. C. Hoffmann, S. Pyon, T. Takayama, H. Takagi, and A. Cavalleri, *Science* **331**, 189 (2011).
 - [14] R. Mankowsky, A. Subedi, M. Först, S. Mariager, M. Chollet, H. Lemke, J. Robinson, J. Glowia, M. Minitti, A. Frano, *et al.*, *Nature* **516**, 71 (2014).
 - [15] W. Hu, S. Kaiser, D. Nicoletti, C. R. Hunt, I. Gierz, M. C. Hoffmann, M. Le Tacon, T. Loew, B. Keimer, and A. Cavalleri, *Nature materials* **13**, 705 (2014).
 - [16] S. Kaiser, C. R. Hunt, D. Nicoletti, W. Hu, I. Gierz, H. Y. Liu, M. Le Tacon, T. Loew, D. Haug, B. Keimer, and A. Cavalleri, *Phys. Rev. B* **89**, 184516 (2014).
 - [17] M. Mitrano, A. Cantaluppi, D. Nicoletti, S. Kaiser, A. Perucchi, S. Lupi, P. Di Pietro, D. Pontiroli, M. Riccò, S. R. Clark, *et al.*, *Nature* **530**, 461 (2016).
 - [18] A. Cavalleri, *Contemporary Physics* **59**, 31 (2018).
 - [19] The populations of the valleys are altered in the presence of a nonzero superconducting gap, thus preventing Pauli blocking.
 - [20] V. Galitskii, S. Goreslavskii, and V. Elesin, *Zh. Eksp. Teor. Fiz.* **57**, 207 (1969).
 - [21] V. Elesin, *Sov. Phys. JETP* **32**, 328 (1971).
 - [22] V. Galitskii, V. Elesin, and Y. V. Kopaev, *ZhETF Pis. Red.* **18**, 50 (1973).
 - [23] D. Kirshnits, *ZhETF Pis. Red.* **17**, 379 (1973).
 - [24] V. Elesin, *Zh. Eksp. Teor. Fiz.* **65**, 2343 (1973).
 - [25] G. Goldstein, C. Aron, and C. Chamon, *Phys. Rev. B* **91**, 054517 (2015).
 - [26] A. H. Castro Neto, F. Guinea, N. M. R. Peres, K. S. Novoselov, and A. K. Geim, *Rev. Mod. Phys.* **81**, 109 (2009).
 - [27] D. Xiao, G.-B. Liu, W. Feng, X. Xu, and W. Yao, *Phys. Rev. Lett.* **108**, 196802 (2012).
 - [28] H. Zeng, J. Dai, W. Yao, D. Xiao, and X. Cui, *Nature nanotechnology* **7**, 490 (2012).
 - [29] K. F. Mak, K. He, J. Shan, and T. F. Heinz, *Nature nanotechnology* **7**, 494 (2012).
 - [30] T. Cao, G. Wang, W. Han, H. Ye, C. Zhu, J. Shi, Q. Niu, P. Tan, E. Wang, B. Liu, *et al.*, *Nature communications* **3**, 887 (2012).
 - [31] W. Yao, D. Xiao, and Q. Niu, *Phys. Rev. B* **77**, 235406 (2008).
 - [32] The assumption of spinlessness is made for simplicity but can be relaxed without changing our results—see Supplemental Material.
 - [33] We do not consider a charge density wave instability in the same intervalley, interband channel since the relevant self-consistency equation has an energy denominator of magnitude $|E_{\mathbf{k}2} - E_{\mathbf{k}1}| \gg |E_{\mathbf{k}2} + E_{\mathbf{k}1}|$. Hence, this instability is much weaker than the one towards the superconducting state we discuss in this letter.
 - [34] We neglected excitonic effects, which becomes more accurate for small δ since the effective mass of both electrons and holes, and therefore the excitonic binding energies, are $\propto \delta$.
 - [35] This expression for the time evolution of $\rho(t)$ is not strictly correct, as it does not account for any changes in the quasiparticles of the system. The Keldysh description discussed in the Supplemental Material fixes this shortcoming.
 - [36] R. R. Puri, *Mathematical methods of quantum optics*, Vol. 79 (Springer Science & Business Media, 2001).
 - [37] M. A. Schlosshauer, *Decoherence: and the quantum-to-classical transition* (Springer Science & Business Media, 2007).
 - [38] J. Bardeen, L. N. Cooper, and J. R. Schrieffer, *Phys. Rev.* **108**, 1175 (1957).
 - [39] M. H. Szymańska, J. Keeling, and P. B. Littlewood, *Phys. Rev. Lett.* **96**, 230602 (2006).
 - [40] M. H. Szymańska, J. Keeling, and P. B. Littlewood, *Phys. Rev. B* **75**, 195331 (2007).
 - [41] A. Mitra, *Phys. Rev. B* **78**, 214512 (2008).
 - [42] In the intraband channel, the population difference $1 - n_{\mathbf{k}}^{\alpha\alpha} - n_{\mathbf{k}}^{\alpha\alpha}$ cannot change sign if only one valley is driven.
 - [43] T. G. Pedersen, A.-P. Jauho, and K. Pedersen, *Phys. Rev. B* **79**, 113406 (2009).
 - [44] Note that our results are only quantitatively correct for regions of the phase diagram where the strength of the interactions V is significantly smaller than the width of the electronic bands $\sim t$, i.e., weak coupling.